*Journal of The Electrochemical Society*, 2024 **171** 050555
1945-7111/2024/171(5)/050555/11/$40.00 © 2024 The Electrochemical Society ("ECS"). Published on behalf of ECS by IOP Publishing Limited

# On the Specific Capacity and Cycle Stability of Si@void@C Anode: Effects of Electrolytes

**Mei Luo, Bingyu Liu, Vignyatha Reddy Tatagari, Ziyong Wang, and Leon L. Shaw**[z]

*Department of Mechanical, Materials and Aerospace Engineering, Illinois Institute of Technology, Chicago, Illinois 60616, United States of America*

Electrolytes play a critical role in the formation of stable solid electrolyte interphase (SEI) for Si anodes. This study investigates the impacts of five different electrolytes on the specific capacity and cycle stability of Si-based anodes and confirms the advantages of the second-generation (Gen2) electrolyte over the first-generation (Gen1) electrolyte in the first 200 cycles, beyond which the advantages of Gen2 electrolyte disappear. Addition of more FEC and VC additives to Gen2 electrolyte does not offer significant advantages in the cycle stability and specific capacities. However, very high FEC electrolytes with 20 wt% FEC and 80% dimethyl carbonate exhibits strong dependance on the lithiation cutoff voltage. This electrolyte results in durable SEI layers when the lithiation cutoff voltage is at 0.01 V vs Li/$Li^+$. Furthermore, lowering the lithiation cutoff voltage from 0.1 V to 0.01 V vs Li/$Li^+$ has raised the specific capacity of Si-based anodes, leading to higher specific capacities than those of graphite anodes at the electrode level for 380 cycles investigated in this study. The understandings developed here provide unambiguous guidelines for selection of electrolytes to achieve long cycle stability and high specific capacity of Si-based cells simultaneously in the future.
 [DOI: 10.1149/1945-7111/ad4f21]

Manuscript submitted February 9, 2024; revised manuscript received May 17, 2024. Published May 30, 2024.

Supplementary material for this article is available online

It is well-known that a challenge for silicon anode application is the unstable solid electrolyte interphase (SEI) at Si anodes, i.e., the SEI layer is supposed to be formed on first few charge/discharge cycles and then be self-terminating; but in reality, the reduction of the electrolyte cannot be suppressed completely and the repeated volume expansion and shrinkage of Si anodes during cycles can induce repeated fracture and reformation of the SEI layer, both of which harm the reversibility and cycle life of Si-based Li-ion batteries.[1,2] Various strategies have been explored in electrolyte development to address SEI-related issues. These strategies can be broadly categorized as follows: (i) forming a durable SEI layer in the first several charge/discharge cycles to minimize further reduction of electrolytes in subsequent cycles,[3–7] (ii) forming a highly elastic and robust SEI layer to limit the volume expansion of Si anodes and thus improve the cycle stability,[8,9] and (iii) forming a SEI layer that allows Si particles to expand and shrink inside the SEI layer because of the weak bonding between the SEI layer and the lithiated Si core.[10]

Electrolyte additives, based on strategy (i), are always used to improve the stability of the SEI layer and thus enhance the cycle life.[3–7] Fluoroethylene carbonate (FEC), a standard additive for Si anodes, has been found to improve the cell performance and aging life substantially.[5,7,11–14] Vinylene carbonate (VC), helping to form passivation layer at graphite (Gr) anodes,[7,15] has also been studied frequently for Si anodes and proved to form a flexible and stable SEI layer on the surface of Si anodes.[5,7,13] It has been reported that the SEI derived from an ethylene carbonate (EC)-dimethyl carbonate (DMC)-based electrolyte with FEC additive is much thinner than the SEI derived from the counterpart electrolyte without FEC.[16] Further, the SEI layers thicken during lithiation and become thinner during delithiation, i.e., thickening/thinning is reversible with cycling for both electrolytes with and without FEC.[16] With the aid of cryogenic electron microscopy it has been uncovered that the SEI derived from an EC-diethyl carbonate (DEC)-based electrolyte has a bilayer structure with amorphous $Li_xSiO_y$ as the inner layer and a lithium ethylene decarbonate (LEDC) plus $Li_2O$ as the outer layer.[17] This SEI bilayer is not stable and completely delithiated in the delithiation process. In contrast, the SEI derived from EC-DEC with 10% FEC additive has different chemical species with the outer layer composed of polycarbonates arising from VC polymerization. This poly (VC) layer is stable electrochemically against oxidation during delithiation.[17] Further, this poly(VC) layer possesses elastomeric properties, offering mechanical stability to accommodate some volume expansion of Si particles during lithiation.[17] Because of these electrochemical and mechanical stabilities, electrolytes with FEC provide much better cycle stability than the counterparts without FEC. It has been found that additive amount affects the capacity retention significantly, and 10 wt% VC can lead to better cell capacity retention than 10 wt% FEC for a blended Si-Gr electrode,[7] which is likely due to the higher VC molarity or a large amount of Gr in the electrode. It has been revealed that VC-derived SEI layers are more flexible to survive the large volume change of nano-Si anodes, whereas FEC-derived SEI layers offer superior conductivity.[13] It is generally accepted that VC-derived SEIs, rich of polycarbonates, have a high reversibility and FEC-derive SEIs which are rich in LiF have better conductivity.[13,18]

In accordance with strategy (ii), the localized high concentration electrolytes (LHCEs), based on lithium bis(fluorosulfony)imide (LiFSI) salt dissolved in triethyl phosphate (TEP) solvent, bis (2,2,2-trifluoroethyl) ether (BTFE) dilute solvent and FEC additive, have been shown to be capable of forming a mechanically robust and LiF-rich SEI which can greatly suppress the swelling of Si-based electrodes and lead to capacity retention of 89.8% after 600 cycles of a commercial Si/Gr composite.[8] In contrast, the capacity of the same electrode drops to zero after 300 cycles for the control electrolyte (1 M $LiPF_6$ in EC/DEC in 3:7 w/w with 10 wt% FEC).[8] Another study using a cyclic phosphate and hydrofluoroether-based electrolyte[9] has revealed that a highly elastic and robust inorganic-polymeric SEI, mainly composed of LiF, $Li_2O$, $Li_xPO_y$, sulfur compounds and polyphosphoesters, can be generated. This SEI allows a micro-sized Si-based electrode to retain 83.1% capacity over 200 cycles with a high average coulombic efficiency (CE) of ~99.9%, whereas the electrolyte of 1 M $LiPF_6$ in EC/DMC with 5 vol% FEC can only retain 31.8% capacity over 200 cycles with highly fluctuated CE.[9]

A good example of strategy (iii) is the recent report using 2 M $LiPF_6$ in a 1:1 v/v mixture of tetrahydrofuran (THF) and 2-methyltetrahydrofuran (MTHF) electrolyte[10] which can lead to the formation of a bilayer SEI, i.e., a high-modulus LiF inner layer in direct contact with the lithiated Si particles and a thin outer layer of an organic shell in contact with the liquid electrolyte. This bilayer SEI has a low adhesion to lithiated Si particles because of the high-purity LiF inner layer and thus allows the Si core to expand and shrink within the SEI shell during charge/discharge cycles.[10] It is demonstrated that this THF-MTHF-based electrolyte can enable 400

[z]E-mail: lshaw2@iit.edu

cycles of a micro-sized Si electrode (particle size >10 $\mu$m) with 90% capacity retention. In contrast, 1 M $LiPF_6$ in EC/DMC electrolyte leads to loss of 40% capacity in 20 cycles and 92% capacity in 50 cycles for the same Si electrode.[10]

In this study, we have investigated the effects of five (5) electrolytes on the cycle stability and specific capacity of Si@void@C anodes. The electrolytes studied are summarized in Table I, including: (i) the first generation electrolyte (Gen1) for Si-based anodes,[19] denoted as E1 electrolyte in this study; (ii) Gen2 electrolyte for Si-based anodes,[19] termed as E2 hereafter; (iii) high FEC and VC electrolyte containing 1 M $LiPF_6$ salt in EC/DMC (3:7 v/v) with 10 vol% FEC and 5 vol% VC, denoted as E3; (iv) high VC electrolyte containing 1 M $LiPF_6$ salt in EC:DMC (3:7 v/v) with 10 vol% VC, referred to as E4; and (v) very high FEC electrolyte containing 1 M $LiPF_6$ salt in a mixture of FEC:DMC (1:4 w/w), termed as E5 in this study. E3 has not been studied previously, while E5 has been reported to be able to significantly improve the cycle stability of Si-based anodes over EC/DMC-based electrolytes because E5 generates SEI layers with a higher LiF content than EC/DMC-based electrolyte.[20] In addition, it is found that the cycle stability derived from E5 is strongly depending on charge/discharge protocols.[20] By investigating these 5 electrolytes with only one type of Si anode (i.e., Si@void@C to be explained in the Experimental section), the effects of these different electrolytes on the cycle stability and specific capacity of Si anodes can be compared directly to enhance our understanding of the functionalities of each electrolyte and provide unambiguous guidelines for selection of proper electrolytes to achieve long cycle stability and high specific capacity of Si anodes simultaneously.

## Experimental

Si@void@C powder was synthesized using the procedure established in previous studies.[21,22] Briefly, the synthesis method consisted of three major steps. The first step was high-energy ball milling of micron-sized Si powder (99.5% purity, 325 mesh, Sigma Aldrich) using a Szegvari attritor mill under an Ar atmosphere to produce nanostructured Si particles. The second step was carbonization treatment by converting polyacrylonitrile (PAN, average molecular weight 150,000, Sigma-Aldrich) to carbon to form carbon-encapsulated nanostructured Si particles, denoted as Si@C. The third step was partial etching of the nanostructured Si core inside Si@C particles using a 0.5 M sodium hydroxide (NaOH, 97.0%, Sigma-Aldrich) solution to create the final Si@void@C particles which contain an outer carbon shell with inner Si nanoclusters, nano-channel-shaped voids, and internal carbon networks, as shown in Figs. S1 and S2. In addition, based on the previous evaluation,[21,22] the weight ratio of the inner Si nanoclusters to the outer C shell plus internal carbon networks is 62 to 38 and the volume fraction of the nano-channel-shaped voids inside Si@void@C particles is ~46%.

Si@void@C powder described above was used as active material in this study. The slurry contained 60 wt% Si@void@C, 20 wt% carbon black (CB, MTI Super P carbon black >99%), and 20 wt% poly(acrylicacid) (PAA, Sigma-Aldrich) with N-methyl-pyrrolidone (NMP) as solvent. The homogeneous slurry, obtained using a Thinky Mixer, was blade casted (200 $\mu$m wet thickness) on a copper foil and vacuum-dried at 120 °C for 12 h. The dried electrode of this composition is denoted as 6:2:2 electrode. In some cases, the electrode with 80 wt% Si@void@C, 10 wt% CB and 10 wt% PAA (termed as 8:1:1 electrode) were fabricated. Half cells, using the dried Si@void@C electrode with a Li chip as counter electrode, were fabricated as CR2032 coin cell format in a glovebox filled with Ar (99.999% purity). The mass loading of active material was about 1.44 mg $cm^{-2}$ for both 6:2:2 and 8:1:1 electrodes, and five different electrolytes investigated have been summarized in Table I.

Neware battery testers were used to evaluate charge/discharge performance using different protocols. The details of charge/discharge protocol three (P3) are as follows. It was comprised of three constant-current constant-voltage (CCCV) lithiation processes (called "discharge" in this study) at the current density of 0.05 A $g^{-1}$, 0.1 A $g^{-1}$ and 0.5 A $g^{-1}$ for the 1st, 2nd and 3rd formation cycles, respectively, until the Si@void@C electrode potential reached 0.1 V vs $Li/Li^+$, followed by potentiostatic hold lithiation at 0.1 V until the current density became 0.005 A/g. After CCCV lithiation, delithiation (termed "charge") was performed using CC process with the current density of 0.05 A $g^{-1}$, 0.1 A $g^{-1}$ and 0.5 A $g^{-1}$ for the 1st, 2nd and 3rd formation cycles, respectively, until the Si@void@C electrode potential reached 1.0 V vs $Li/Li^+$. Once the three formation cycles were completed, service cycles were conducted for 400 or 600 cycles with CCCV to lithiate Si@void@C at 1 A $g^{-1}$ to 0.15 V vs $Li/Li^+$ and hold at 0.15 V until the current density became 0.05 A/g. The delithiation of Si@void@C was then performed at CC mode at 0.5 A $g^{-1}$ to 1.0 V vs $Li/Li^+$. Other charge/discharge protocols (P4, P5 and P6) are similar to P3 but with different cutoff voltages and their details are summarized in Table II. All specific capacities in this study were computed based on the weight of Si@void@C in the electrode unless stated otherwise.

For the cells with P3 protocol, electrochemical impedance spectroscopy (EIS) data was collected using PARSTAT 4000 (Princeton Applied Research) before and after formation cycles as well as after every 200 service cycles. The amplitude was 10 mV and the frequency range was 100 kHz to 0.1 Hz. The spectrum was taken at the end of the delithiated state. The collected EIS were fitted using ZSimpWin software. The EIS data for other cells were also collected after the cells being subjected to predetermined charge/discharge cycles using the same EIS parameters as the cells with P3 protocol.

## Results and Discussion

***Effects of Gen1 and Gen2 electrolytes.***—Figure 1 reports the specific capacity of Si@void@C half cells (6:2:2 electrodes) as a function of cycle number with E1, E2, E3 and E4 electrolytes and charged/discharged with P3 protocol. To evaluate the intrinsic capacity, the initial cycle and about every 100 cycles of all cells were charged/discharged between 0.01 V–1.0 V vs $Li/Li^+$, as described in Fig. 1. A clear trend regarding cycling performance can be observed that the cells with Gen2 electrolyte have higher specific capacities (~40 mAh $g^{-1}$ higher) than the cells with Gen1 electrolyte in the first 200 cycles. However, from 200 to 300 cycles the specific capacities from these two types of cells become similar, whereas from 300 to 400 cycles the cells with Gen1 electrolyte start to outperform the cells with Gen2 electrolyte.

To understand the source(s) of capacity decay better, the charge/discharge curves of cells with E1 and E2 electrolytes (Figs. 2a and 2b) are examined. Since lithiation is conducted in the CCCV mode, the total specific capacity can be divided in two segments with

**Table I. Electrolytes investigated.**

| Electrolyte ID | Electrolyte composition | Comments |
|---|---|---|
| E1 | 1 M $LiPF_6$ in EC: DEC (3:7 v/v) + 10 vol% FEC + 1 vol% VC | Gen1 electrolyte for Si anodes |
| E2 | 1 M $LiPF_6$ in EC: DMC (3:7 v/v) + 10 vol% FEC + 1 vol% VC | Gen2 electrolyte for Si anodes |
| E3 | 1 M $LiPF_6$ in EC: DMC (3:7 v/v) + 10 vol% FEC + 5 vol% VC | High FEC and VC electrolyte |
| E4 | 1 M $LiPF_6$ in EC: DMC (3:7 v/v) + 10 vol% VC | High VC electrolyte |
| E5 | 1 M $LiPF_6$ in FEC: DMC (1:4 w/w) | Very high FEC electrolyte |

**Table II. Charge/discharge protocols used in this study.**

| Protocol ID | Formation cycles | Service cycles |
|---|---|---|
| P3 (CCCV) | a) Lithiate Si@void@C at 0.05 A/g to 0.1 V vs Li/Li$^+$ and hold at this potential until the current density becomes 0.005 A g$^{-1}$. Delithiate the cell at 0.05 A/g to 1.0 V.<br>b) Lithiate Si@void@C at 0.1 A g$^{-1}$ to 0.1 V vs Li/Li$^+$ and hold at this potential until the current density becomes 0.005 A g$^{-1}$. Delithiate the cell at 0.1 A g$^{-1}$ to 1.0 V.<br>c) Lithiate Si@void@C at 0.5 A g$^{-1}$ to 0.1 V vs Li/Li$^+$ and hold at this potential until the current density becomes 0.005 A g$^{-1}$. Delithiate the cell at 0.5 A/g to 1.0 V. | Lithiate at 1.0 A g$^{-1}$ to 0.15 V vs Li/Li$^+$ and hold at this potential until the current density becomes 0.05 A/g.<br>Delithiate the cell at 0.5 A g$^{-1}$ to 1.0 V. Cycle for 400 or 600 times. |
| P4 (CCCV) | Same as P3 (CCCV) | Lithiate at 1.0 A g$^{-1}$ to 0.1 V vs Li/Li$^+$ and hold at this potential until the current density becomes 0.05 A/g.<br>Delithiate the cell at 0.5 A g$^{-1}$ to 1.0 V. Cycle for 300 or 380 times. |
| P5 (CCCV) | a) Lithiate Si@void@C at 0.05 A/g to 0.01 V vs Li/Li$^+$ and hold at this potential until the current density becomes 0.005 A g$^{-1}$. Delithiate the cell at 0.05 A g$^{-1}$ to 1.0 V.<br>b) Lithiate Si@void@C at 0.1 A g$^{-1}$ to 0.01 V vs Li/Li$^+$ and hold at this potential until the current density becomes 0.005 A g$^{-1}$. Delithiate the cell at 0.1 A g$^{-1}$ to 1.0 V.<br>c) Lithiate Si@void@C at 0.5 A g$^{-1}$ to 0.01 V vs Li/Li$^+$ and hold at this potential until the current density becomes 0.005 A g$^{-1}$. Delithiate the cell at 0.5 A g$^{-1}$ to 1.0 V.<br>d) Lithiate Si@void@C at 0.5 A g$^{-1}$ to 0.1 V vs Li/Li$^+$ and hold at this potential until the current density becomes 0.005 A g$^{-1}$. Delithiate the cell at 0.5 A g$^{-1}$ to 1.0 V. | Lithiate at 1.0 A g$^{-1}$ to 0.1 V vs Li/Li$^+$ and hold at this potential until the current density becomes 0.05 A g$^{-1}$.<br>Delithiate the cell at 0.5 A g$^{-1}$ to 1.0 V. Cycle for 300 or 380 times. |
| P6 (CCCV) | a) Lithiate Si@void@C at 0.05 A g$^{-1}$ to 0.01 V vs Li/Li$^+$ and hold at this potential until the current density becomes 0.005 A g$^{-1}$. Delithiate the cell at 0.05 A g$^{-1}$ to 1.0 V.<br>b) Lithiate Si@void@C at 0.1 A g$^{-1}$ to 0.01 V vs Li/Li$^+$ and hold at this potential until the current density becomes 0.005 A g$^{-1}$. Delithiate the cell at 0.1 A g$^{-1}$ to 1.0 V.<br>c) Lithiate Si@void@C at 0.5 A g$^{-1}$ to 0.01 V vs Li/Li$^+$ and hold at this potential until the current density becomes 0.005 A g$^{-1}$. Delithiate the cell at 0.5 A g$^{-1}$ to 1.0 V. | Lithiate at 0.5 A g$^{-1}$ to 0.01 V vs Li/Li$^+$ and hold at this potential until the current density becomes 0.05 A g$^{-1}$.<br>Delithiate the cell at 0.5 A g$^{-1}$ to 1.0 V. Cycle for 300 or 380 times. |

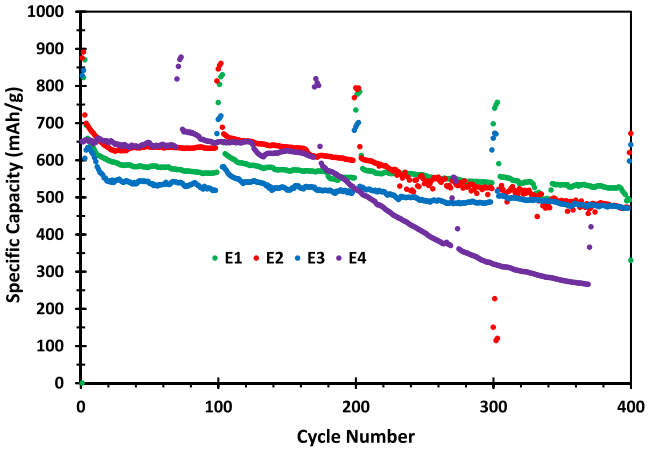


**Figure 1.** Cycle stability comparison of Si@void@C half cells with 6:2:2 electrodes and different electrolytes (i.e., E1, E2, E3 and E4 electrolytes as color coded). All cells are charged/discharged with P3 protocol. However, at the 1st, 100th, 200th, 300th and 400th cycles, E1, E2 and E3 cells are charged/discharged between 0.01 V–1.0 V vs Li/Li$^+$, whereas at the 1st, 75th, 175th, 275th, and 375th cycles, E4 cell is charged/discharged between 0.01 V–1.0 V vs Li/Li$^+$ to evaluate the intrinsic capacities of these cells.

one from the constant current (CC) lithiation and the other from the constant voltage (CV) lithiation (Fig. S3). As shown in Table I, the CC segment for P3 has a high current density (1 A g$^{-1}$), and thus the specific capacity from this segment is very sensitive to the cell impedance, i.e., the larger the cell impedance, the more polarization and thus the lower specific capacity. Examination of Figs. 2 and S3 unambiguously reveals that the specific capacity from the CC segment decreases with increasing cycle numbers for both Gen1 and Gen2 cells, suggesting that the cell impedance increases as cycle number increases. In addition, the specific capacity of the CC segment from Gen2 cells is larger than that from Gen1 cells at the same cycle number, suggesting that Gen2 cells have lower cell impedance than Gen1 cells, which is consistent with the impedance measurements (to be discussed later). The specific capacity from the CV segment, however, stays more or less constant over cycles for both cells, indicating that the specific capacity available from Si@void@C electrodes have not changed much if the current density is low (decreasing from 1 A g$^{-1}$ to 0.05 A g$^{-1}$).

Examination of the EIS data, Fig. 3a, confirms that the impedance is lower for the cell with Gen2 electrolyte than that of the cell with Gen1 electrolyte after 200 cycles. These results are consistent with the work reported elsewhere that the EC/DEC electrolyte exhibit less conductivity than EC/DMC electrolyte at room temperature.[23] Using the equivalent circuit of R(CR)(CR)(C(RW)) shown in Fig. 3b, the total impedance, $R_{total}$, can be decomposed into four components with $R_e$ standing for the electrolyte resistance, $R_{sei}$ the SEI layer resistance, $R_{int}$ the contact resistance of interphases, and $R_{ct}$ the charge transfer resistance. $CPE_{sei}$, $CPE_{int}$ and $CPE_{ct}$ are the capacitances of the constant phase elements associated with the corresponding resistances mentioned above. $W_o$ is the Warburg impedance representing the diffusion resistance of Li$^+$ into the active material. The EIS fitted results for

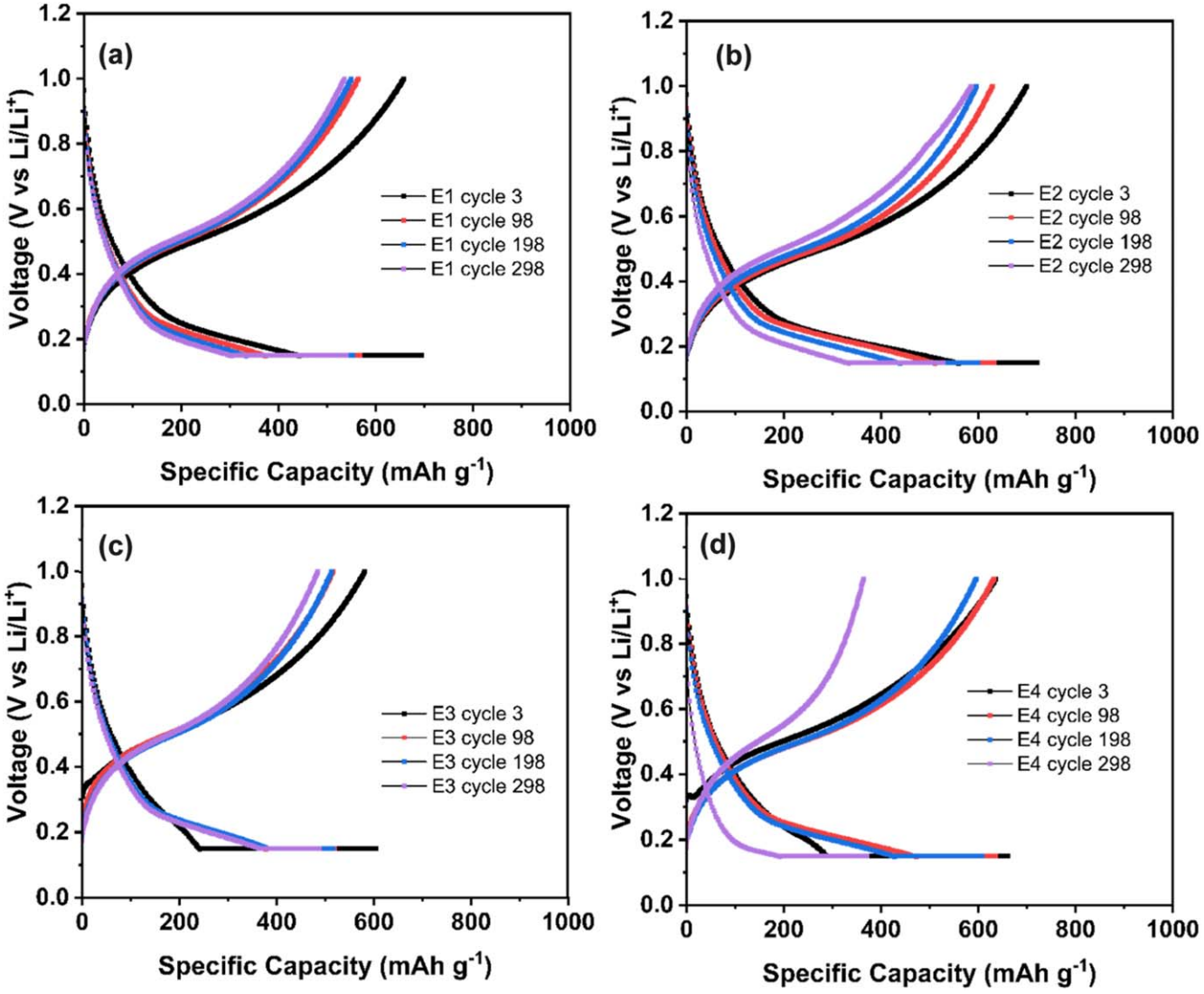


**Figure 2.** Charge/discharge curves of selected cycles for Si@void@C half cells (6:2:2 electrodes) with: (a) E1, (b) E2, (c) E3 and (d) E4 electrolytes. All cells are charged/discharged with P3 protocol.

cells with Gen1 and Gen2 electrolytes after 200 and 400 cycles are summarized in Table III, which shows that the cell with Gen2 electrolyte has lower $R_e$, $R_{sei}$, $R_{int}$ and $R_{ct}$ when compared with those of the cell with Gen1 electrolyte after 200 cycles. However, all of these impedances jump substantially for the cell with Gen2 electrolyte after 400 cycles, leading to a huge increase in $R_{total}$. In contrast, the cell with Gen1 electrolyte only exhibits impedance increase in $R_e$ and $R_{int}$ after 400 cycles with a much smaller increase in $R_{total}$. Noted that the specific capacity changes over cycles for cells with E1 and E2 electrolytes are in good accordance with their inverse cell impedance changes over cycles, indicating that polarization induced by high impedance is one of the key factors controlling the specific capacity of Si@void@C electrodes.

The different behaviors observed for cells with E1 and E2 electrolytes are no doubt due to the solvent change from DEC to DMC since everything else is the same. The present study uncovers that Gen1 electrolyte creates higher impedances initially and thus lower specific capacity from 1 to 200 cycles, but the impedances show little or no increase after large cycle numbers (from 200 to 400 cycles). In contrast, the cell with Gen2 electrolyte has low initial impedances which, however, increase dramatically after 400 cycles, leading to lower specific capacities than the cell with Gen1 electrolyte from 300 to 400 cycles. The trend of the impedance change is interestingly consistent with a previous study,[24] showing that the SEI layers have the same chemical structure, mainly composed of $(CH_2OCOOLi)_2$, for both EC/DEC and EC/DMC electrolytes at the 1st cycle. However, the EC/DMC cell displays LiF formation after 10 cycles, whereas the EC/DEC cell exhibits no change in the SEI chemical structure, suggesting that the SEI derived from EC/DEC-based electrolyte is more stable electrochemically than that from EC/DMC-based electrolyte.

***Effects of high FEC and VC electrolytes.***—The specific capacities of cells with E3 and E4 as a function of cycle number and their representative charge/discharge curves are shown in Figs. 1 and 2, respectively, in comparison with those of cells having E1 and E2 electrolytes. The specific capacity contributions from the CC and CV segments for E3 and E4 cells are very different from those for E1 and E2 cells (Fig. S3). In the initial cycles (such as the 3rd cycle) both E3 and E4 cells exhibit smaller capacity contributions from the CC segment when compared with those from the CV segment. This indicates that E3 and E4 cells have high polarization when the current density is high (at 1 A $g^{-1}$ for the CC segment), mostly due to the high impedance of E3 and E4 cells which is consistent with the fact that both E3 and E4 electrolytes contain high FEC and VC contents. Interestingly, as cycle number increases from 3 cycles to 98 cycles, the specific capacity from the CC segment becomes larger than that from the CV segment for both E3 and E4 cells. The precise

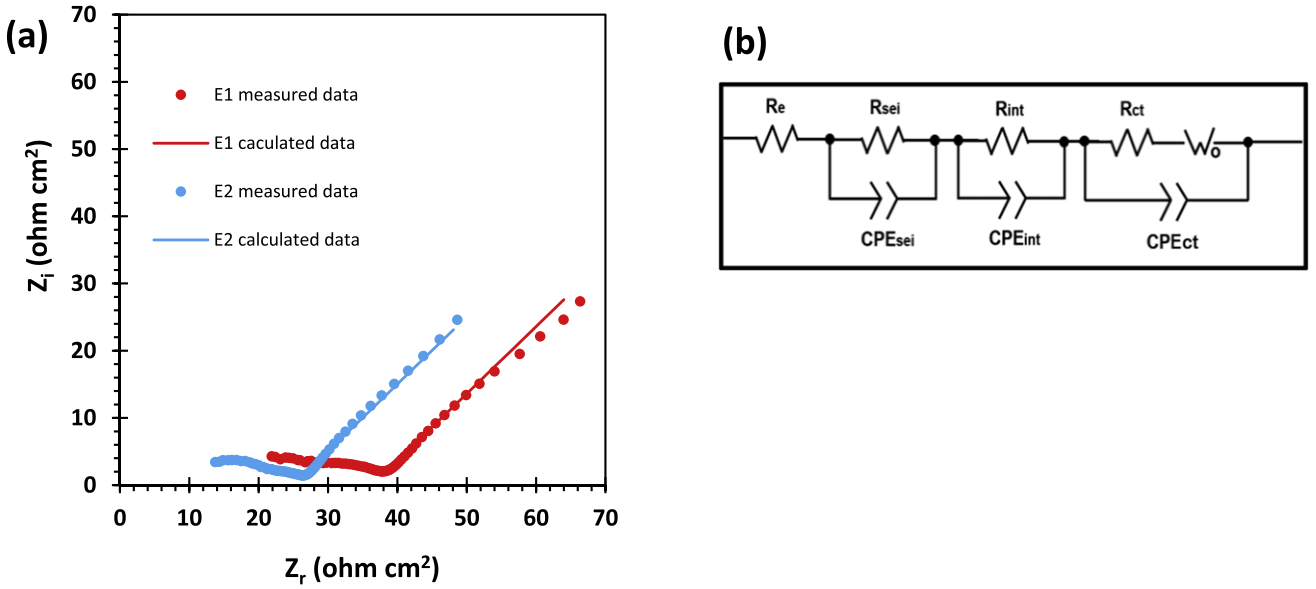


**Figure 3.** (a) Electrochemical impedance spectra of Si@void@C half cells (6:2:2 electrodes) with E1 and E2 electrolytes after 200 service cycles as indicated. Both cells are charged/discharged with P3 protocol. Dots are measured data, while lines are fitted data using the equivalent circuit of R(CR)(CR)(C(RW)) shown in (b).

**Table III. Impedance data for M cells with 6:2:2 electrode.[a)].**

| Sample ID | Electrolyte (cycle #; charge/discharge protocol) | $R_e$ ($\Omega$.cm$^2$) | $R_{sei}$ ($\Omega$.cm$^2$) | $R_{int}$ ($\Omega$.cm$^2$) | $R_{ct}$ ($\Omega$.cm$^2$) | $R_{total}$ ($\Omega$.cm$^2$) |
|---|---|---|---|---|---|---|
| M1 | E1 (200 cycles; P3) | 18.60 | 7.43 | 5.08 | 5.37 | 36.48 |
| M2 | E1 (400 cycles; P3) | 24.16 | 5.57 | 9.44 | 4.98 | 44.15 |
| M3 | E2 (200 cycles; P3) | 12.25 | 6.52 | 3.27 | 4.35 | 26.42 |
| M4 | E2 (400 cycles; P3) | 23.70 | 9.89 | 15.53 | 11.19 | 60.32 |
| M5 | E3 (200 cycles; P3) | 12.72 | 7.81 | 5.12 | 4.45 | 30.12 |
| M6 | E3 (600 cycles; P3) | 47.57 | 79.11 | 29.82 | 38.14 | 194.64 |
| M7 | E4 (200 cycles; P3) | 13.70 | 6.96 | 13.16 | 20.78 | 54.63 |
| M8 | E4 (400 cycles; P3) | 30.99 | 11.70 | 9.78 | 34.20 | 86.67 |
| M9 | E4 (600 cycles: P3) | 43.20 | 23.38 | 13.93 | 36.70 | 117.21 |

a) The impedances of the cells with E1 and E2 at 600 cycles and E3 at 400 cycles were not measured.

reason for this phenomenon is not clear yet but possibly due to participation in redox reactions of more activated Si@void@C particles as cycle number increases. It is noted that E3 cells have stable specific capacity contributions from both CC and CV segments as cycle number increases from 98 to 398 cycles. Thus, E3 cells have good capacity retention, but with the lowest specific capacities among E1, E2, E3 and E4 cells (Fig. 1). These phenomena can be explained by high FEC and VC contents in E3 electrolyte, which leads to high impedance but durable SEI layers and thus low specific capacities but good capacity retention.

The EIS measurements of cells with E3 and E4 after 200 cycles are shown in Fig. 4 along with the fitted data. Furthermore, the fitted impedance data for cells with E3 and E4 are also summarized in Table III. When comparing the specific capacities and impedance data among the cells with E1, E2, E3 and E4, several interesting but complicated trends are noted. First, E4 electrolyte leads to the highest impedance among all cells after 200 cycles, but does not result in the lowest specific capacity. Instead, the cell with E4 exhibits specific capacities as high as the cell with E2 from 20 to 200 cycles, indicating that the specific capacities are not 100% dictated by the cell impedance only (to be discussed further later). Second, E3 electrolyte results in the second lowest impedance among all cells, but the cell with E3 has the lowest specific impedance, again indicating that the specific capacities are not 100% dictated by the cell impedance only. Third, the cell impedance increases as the cycle number increases for all cells.

It is known that the specific capacity of Si anodes can be controlled by multiple factors, including (i) the cell impedance, (ii) the electrode material utilization,[25,26] and (iii) the charge/discharge conditions.[2,21,22] The capacity decay at a given charge/discharge condition could be a result either from cell impedance growth and/or the electrode degradation. Examination of coulombic efficiency (CE) as a function of cycle numbers could help identify the source(s) of the capacity decay. As shown in Fig. 5, all cells, regardless of their electrolytes, have their average CE below 99.6%. Specifically, cells with E1 have the lowest average CE at 99.35%, suggesting a less passivated SEI layer formed by E1 electrolyte compared to E2 electrolyte. In addition, while cells with E3 electrolyte display the lowest specific capacity in first 200 cycles (Fig. 1), they exhibit the highest average CE at 99.45%, suggesting a role of high FEC and VC concentrations in forming a durable SEI layer. These trends are consistent with the stable specific capacity contributions from both CC and CV segments for cells with E3 electrolyte as cycle number increases from 98 to 398 cycles shown in Fig. S3. It should be pointed out that previous studies[5,7,13] have shown that VC can form a flexible and stable SEI layer on Si anodes. FEC-derived SEIs can also accommodate some volume expansion of Si particles during lithiation although FEC-derived SEIs have better conductivity than the counterparts derived from VC.[17] As such, it can be expected that the SEIs derived from E3 will be more mechanically durable than SEIs derived from E1 and E2 because E3 contains higher VC concentrations than E1 and E2 while having the same FEC contents

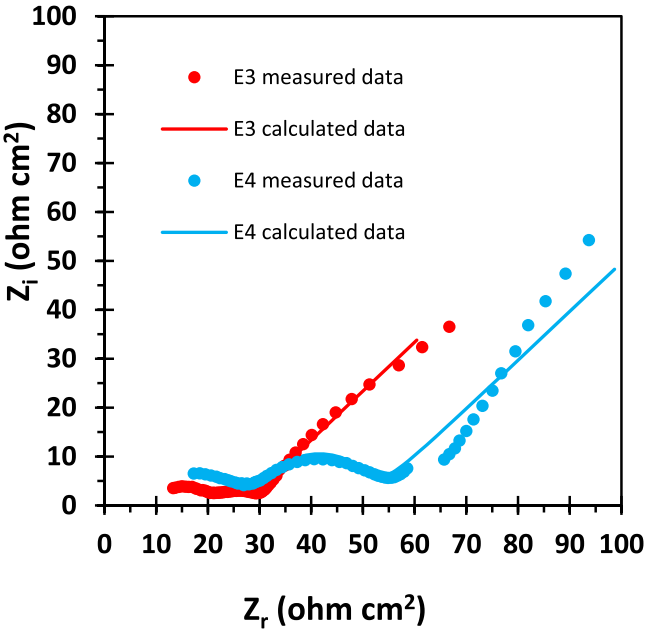


**Figure 4.** (a) Electrochemical impedance spectra of Si@void@C half cells (6:2:2 electrodes) with E3 and E4 electrolytes after 200 service cycles as indicated. Both cells are charged/discharged with P3 protocol. Dots are measured data, while lines are fitted data using the equivalent circuit of R (CR)(CR)(C(RW)) shown in Fig. 3b.

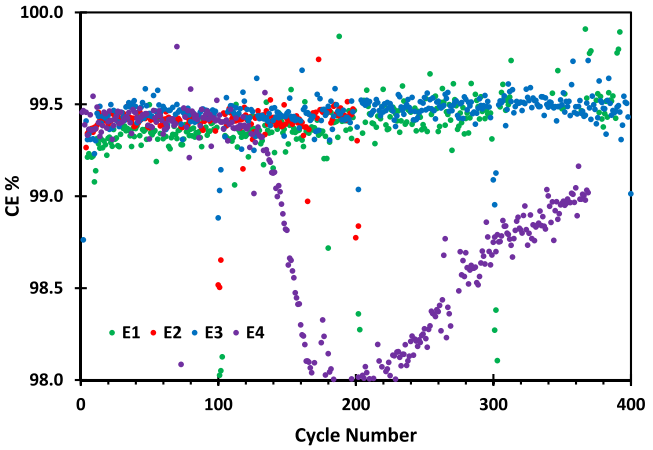


**Figure 5.** Coulombic efficiency (CE) of Si@void@C half cells (6:2:2 electrodes) with E1, E2, E3 and E4 electrolytes as a function of service cycles. All cells are charged/discharged with P3 protocol.

(Table I). Note that the volume expansion of Si@void@C electrodes under the charge/discharge condition used here[21] can cause fracture and gradual loss of some Si@void@C particles in participation in electrochemical reactions. The higher CE exhibited by cells with E3 electrolyte than cells with E1 and E2 is in good accordance with the expectation of their more durable SEI layers and fewer fracture events and less loss of Si@void@C particles per cycle.

For a given charge/discharge condition, the specific capacity of Si@void@C will be determined by the cell impedance and the integrity of the Si@void@C anode. This expectation is consistent with the finding that cells with E2 have the highest specific capacity among cells with E1, E2 and E3 (Fig. 1) because cells with E2 have the lowest impedance after 200 cycles (Table III) and thus the smallest polarization. In addition, the order of the cell impedance after 3 formation cycles is found to be E2 ($R_{total} = 22.1\ \Omega.cm^2$) < E1 ($R_{total} = 26.2\ \Omega.cm^2$) < E3 ($R_{total} = 28.4\ \Omega.cm^2$), which is consistent with the order of the delithiation specific capacity at the first service cycle, E2 (702 mAh $g^{-1}$) > E1 (667 mAh $g^{-1}$) > E3 (605 mAh $g^{-1}$). These results indicate that the cell impedance is indeed an important factor dictating the specific capacity of Si@void@C cells. Therefore, it can be concluded that E3 cells have mechanically durable SEI but with high impedance, leading to lower specific capacities but better integrity of electrode materials during cycles. In contrast, E2 cells have the lowest impedance and thus highest specific capacity while its lower average CE (99.42%) in the first 150 cycles compared to E3 cells (99.45%) suggests a less passivated SEI formed with less VC in the electrolyte.

E4 cells have the highest impedance among E1, E2, E3 and E4 cells after 200 cycles (Table III) because E4 cells contain very high VC concentration (10 vol%). This is consistent with the previous study showing VC additive results in durable SEIs with higher impedance than FEC.[13] Because of their high impedance, E4 cells exhibit relatively low specific capacities initially (Fig. 1), but their specific capacities gradually increase after the initial decrease from the first to 10th cycles. The specific capacity increase from the 10th to 42nd cycles is due to the participation of more Si@void@C particles and/or the central portion of large Si@void@C particles in electrochemical reactions as cycle number increases.[22] However, after 42 cycles the specific capacity of E4 cells start to decrease, likely owing to the gradual fracture and loss of some Si@void@C particles in electrochemical reactions. In spite of their highest impedance, E4 cells possess specific capacities as high as E2 cells from 43 to 200 cycles. These complicated phenomena are attributed to the durable VC-derived SEI which minimizes the fracture and loss of Si@void@C particles in electrochemical reactions during cycles as reflected by the high CE (99.41%) of E4 cells in the first 150 cycles. However, beyond 150 cycles the CEs of E4 cells drop substantially (Fig. 5), likely owing to sudden fracture of SEIs after surviving 150 volume expansion/shrinkage cycles. With continued fracturing and reformation of SEIs the specific capacity of E4 cells begins to decrease rapidly beyond 200 cycles (Fig. 1b).

***Effects of very high FEC electrolyte.***—Cells with E5 electrolyte (Table I) are used to study the effect of electrolytes with very high FEC concentrations. The electrodes of these cells contain 80 wt% Si@void@C, 10 wt% CB and 10 wt% PAA (i.e., 8:1:1 electrodes summarized as B cells in Table IV) rather than M cells with E1, E2, E3 and E4 discussed above which have 6:2:2 electrodes (Table III).

**Table IV. Impedance data for B cells with 8:1:1 electrode.**

| Sample ID | Electrolyte (cycle #; charge/discharge protocol) | $R_e$ ($\Omega.cm^2$) | $R_{sei}$ ($\Omega.cm^2$) | $R_{int}$ ($\Omega.cm^2$) | $R_{ct}$ ($\Omega.cm^2$) | $R_{total}$ ($\Omega.cm^2$) |
|---|---|---|---|---|---|---|
| B1 | E1 (30 cycles; P4) | — | — | — | — | 15.21 |
| B2 | E5 (30 cycles; P4) | 4.08 | 3.46 | 3.94 | 10.43 | 21.91 |
| B2’ | E5 (180 cycles; P4) | 6.13 | 5.58 | 6.98 | 23.48 | 42.17 |
| B3 | E1 (30 cycles; P5) | — | — | — | — | 15.81 |
| B4 | E5 (30 cycles; P5) | 4.28 | 11.87 | 4.17 | 4.49 | 24.81 |
| B4’ | E5 (180 cycles; P5) | 6.19 | 5.17 | 7.18 | 16.38 | 34.92 |
| B5 | E5 (30 cycles; P6) | 4.69 | 11.27 | 3.59 | 4.24 | 23.79 |
| B5’ | E5 (180 cycles; P6) | 5.61 | 3.68 | 5.42 | 11.50 | 26.20 |

The specific capacities of B cells with E5 electrolyte (i.e., B2 and B4) as a function of cycle numbers and charge/discharge protocols are shown in Fig. 6 along with B cells having E1 electrolyte (i.e., B1 and B3) for direct comparison. Several prominent trends are noted from Fig. 6. First, B1 cells with E1 electrolyte have lower specific capacities than M1 cells with E1 electrolyte shown in Fig. 1 even though B1 cells have lower lithiation cutoff voltages (P4 protocol) than M1 cells (P3 protocol). These results suggest that Si@void@C particles themselves do not have sufficient electronic conductivity and require addition of high CB concentrations (such as 20 wt% CB in M cells with 6:2:2 electrodes) to offer high electronic conductivity and thus fully utilize the specific capacity of Si@void@C particles. Electrical conductivity measurements via EIS have confirmed that the electrical conductivity of Si@void@C particles is indeed about two orders of magnitude lower than that of CB particles (Table S1). Second, as shown in Fig. 6a, the specific capacity of B1 cells with E1 electrolyte is higher than that of B2 cells with E5 electrolyte. Given that B1 and B2 cells have the same conditions except different electrolytes, it is deduced that the lower specific capacity of B2 cells is due to the high impedance of the cell induced by E5 electrolyte–a very high FEC electrolyte. This deduction is confirmed by EIS measurements. As shown in Fig. 7a and summarized in Table IV, the total resistance of B2 cell after 30 cycles, $R_{total}$, is 21.91 $\Omega.cm^2$ which is larger than the corresponding value of B1 cell ($R_{total} = 15.21\ \Omega.cm^2$). The higher impedance of B2 cell is consistent with the expectation of the very high FEC concentration in E5 electrolyte.

Third, it is interesting to note that the specific capacities of B1 and B2 cells as a function of cycle numbers exhibit a similar trend for P4 charge/discharge protocol (Fig. 6a). However, when charge/discharge protocol changes from P4 to P5, the cycle stability trends of B3 and B4 cells with E1 and E5 electrolytes, respectively, become very different (Fig. 6b). Note that P4 and P5 have the same charge/discharge protocol in service cycles (Table II), but their formation cycles are different. The lower lithiation cutoff voltage in the formation cycles is 0.1 V vs $Li/Li^+$ for P4, whereas it is 0.01 V vs $Li/Li^+$ for P5. The lower cutoff voltage in lithiation of Si@void@C anodes is expected to lead to deeper activation and higher utilization of active materials as well as a thicker and durable SEI. The former could result in higher specific capacities at early stage and the latter could lead to different properties of SEI such as a higher impedance and a stronger mechanical strength. A previous study[20] has revealed that a lower cutoff voltage for E5 electrolyte can result in durable SEI layers and thus better cycle stability. A comparison between Figures 6a and 6b indeed reveals that the specific capacities of Si@void@C electrodes at the first service cycle have increased for both cells with E1 and E5 electrolytes when charge/discharge protocol changes from P4 to P5. A comparison between Figs. 7a and 7b confirms that the impedance increase of B cells with E1 is small (only 3.94% increase from B1 to B3 cells) whereas the corresponding increase of B cells with E5 is large (13.23% increase from B2 to B4 cells) when charge/discharge protocol changes from P4 to P5. Because of more durable SEI layers induced by P5, B4 cell with E5 has displayed much improved cycle stability than B3 cell with E1. Thus, even though B3 cell has a high initial specific capacity (~620 mAh $g^{-1}$), its specific capacity has reduced to only 279 mAh $g^{-1}$ (~45% capacity retention) after 300 cycles (Fig. 6b). In contrast, B4 cell has a relatively low initial specific capacity (~562 mAh $g^{-1}$) but its specific capacity is relatively high at 376 mAh $g^{-1}$ after 300 service cycles (~67% capacity retention) because of its durable SEI layers with higher impedance.

The charge/discharge curves and the specific capacity contributions of B1 to B4 cells are shown in Figs. 8 and S4, respectively. The charge/discharge curves of B1 and B2 cells with P4 protocol look similar except the lower capacity of B2 cells when compared with that of B1 cells. However, when charge/discharge protocol changes from P4 to P5, B3 cells display rapid increase in polarization (Fig. 8c) and fast decay in the specific capacity contribution from the CC segment (Fig. S4) as cycle number increases. In contrast, B4 cells exhibit smaller polarization (Fig. 8d) and slower capacity decay from the CC segment (Fig. S4) as cycle number increases when compared with B3 cells. These results suggest that B4 cells with E5 electrolyte can result in more durable SEI layers when the lithiation cutoff voltage in the formation cycle is decreased to 0.01 V vs $Li/Li^+$. This trend is in good accordance with the previous discussion of Figs. 6 and 7. In contrast, B3 cells with E1 electrolyte display rapid polarization increase and fast capacity decay from the CC segment, most likely owing to the less sensitivity of the SEI layer durability derived from E1 electrolyte to the lithiation cutoff voltage than E5 electrolyte.

***Effects of charge/discharge protocol.***—Figure 6 unambiguously reveals that charge/discharge protocol has significant influence on the specific capacity and cycle stability of Si@void@C anodes. Therefore, the effects of charge/discharge protocol on cells with E5 electrolyte are investigated further. Since Figs. 6 and 7 have shown that lower cutoff voltages in lithiation can generate more durable SEI layers and higher specific capacity, we have designed charge/discharge protocol P6 which is similar to P5 in the formation cycles, but has reduced the cutoff voltage in lithiation to 0.01 V vs $Li/Li^+$ in

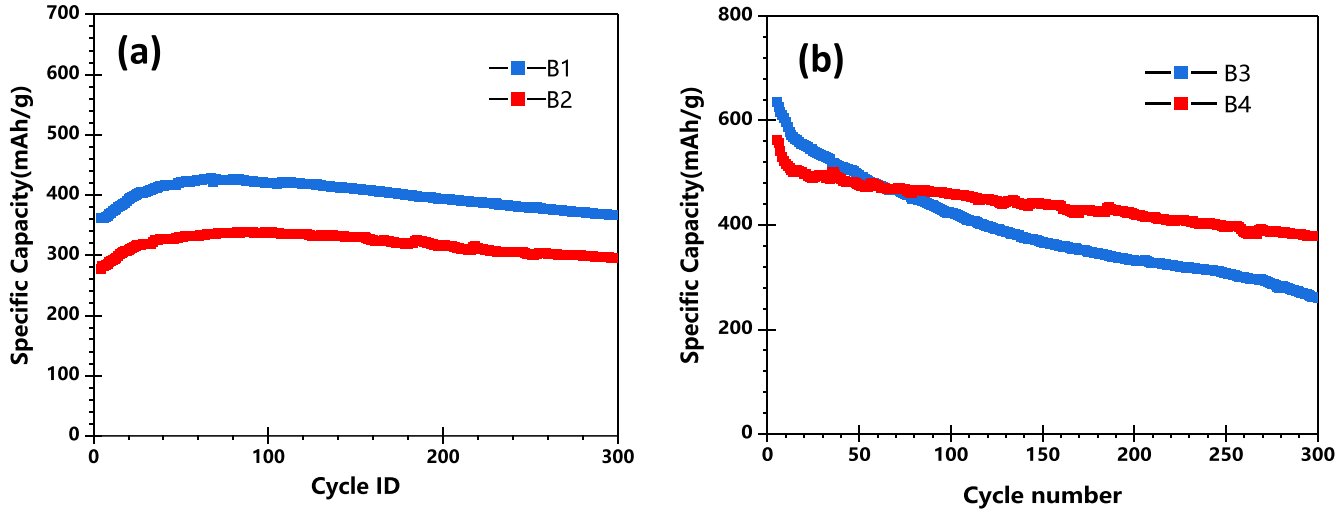


**Figure 6.** Cycle stability comparison of Si@void@C half cells with 8:1:1 electrodes: (a) P4 charge/discharge protocol for both B1 cell with E1 electrolyte and B2 cell with E5 electrolyte, and (b) P5 charge/discharge protocol for both B3 cell with E1 electrolyte and B4 cell with E5 electrolyte. Other conditions are the same for all cells.

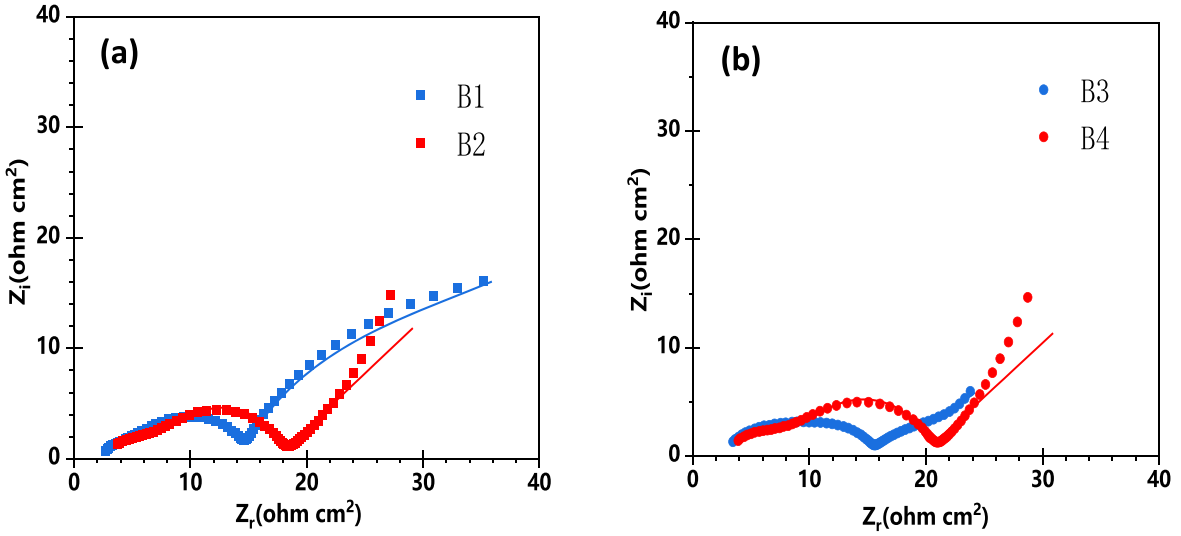


**Figure 7.** Electrochemical impedance spectra: (a) B1 and B2 cells (8:1:1 electrodes) with E1 and E5 electrolyte, respectively, and P4 charge/discharge protocol, and (b) B3 and B4 cells (8:1:1 electrodes) with E1 and E5 electrolyte, respectively, and P5 charge/discharge protocol after 30 service cycles. Dots are measured data, while lines are fitted data using the equivalent circuit of R(CR)(CR)(C(RW)) shown in Fig. 3b.

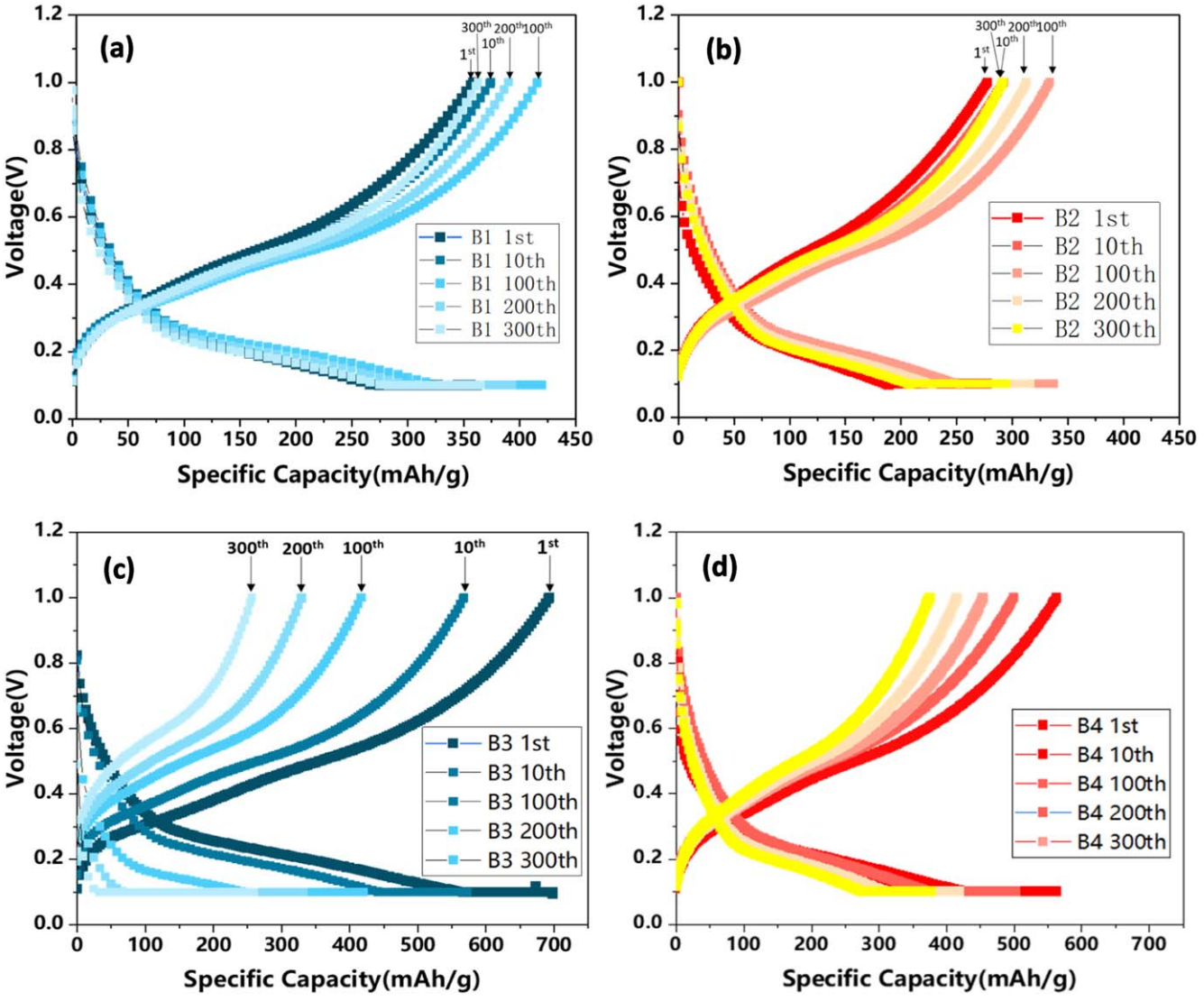


**Figure 8.** Charge/discharge curves of selected cycles for Si@void@C half cells (8:1:1 electrodes) with: (a) B1 cell (E1 electrolyte and P4 protocol), (b) B2 cell (E5 electrolyte and P4 protocol), (c) B3 cell (E1 electrolyte and P5 protocol), and (d) B4 cell (E5 electrolyte and P5 protocol).

service cycles (Table II). Figure 9a compares the specific capacity and cycle stability of B2, B4 and B5 cells with E5 electrolyte and P4, P5 and P6 protocols, respectively. It is interesting to see that B5 cell with P6 protocol not only has the highest initial specific capacity (810 mAh $g^{-1}$), but also possesses the highest final specific capacity (438 mAh $g^{-1}$) after 380 cycles among the three protocols. Thus, lower cutoff voltages in lithiation with E5 electrolyte have provided advantages over higher cutoff voltages by offering higher specific capacity because of the greater utilization of electrode materials as well as the formation of more durable SEI layers and thus less fracture and reformation of SEI layers over 380 cycles.

Examination of the cell impedance provides additional insights into the advantage of P6 protocol. As shown in Fig. 9b, the impedance of B5 cell is the lowest after 180 cycles among the three cells. To understand this phenomenon, the evolutions of cell impedance as a function of cycle number for B2, B4 and B5 cells have been summarized in Table IV. The impedance of B4 cell is higher than that of B2 cell after 30 service cycles because B4 cell has a lower cutoff voltage (0.01 V vs $Li/Li^+$) in the formation cycles than that of B2 cell (0.1 V vs $Li/Li^+$). When the cycle number increases from 30 to 180 (i.e., B2 and B4 change to B2' and B4', respectively, in Table IV), the total resistances of both B2 and B4 cells increase. In particular, the charge transfer resistance, $R_{ct}$, increases substantially for both cells, while the SEI layer resistance, $R_{sei}$, increases slightly for B2 cell and even decreases slightly for B4 cell. The small changes in the SEI layer resistance suggests repeated fracture and formation of the SEI layer as cycles proceed. Since the old SEI layer is replaced by the new SEI layer, the SEI layer resistance would not change much as cycles proceed. However, the charge transfer resistance increases substantially because the accumulation of fractured SEI layers has dramatically increased the travel distance of Li ions from the fractured SEI layers/electrolyte interface to the Si core in the Si@void@C particle.

In contrast to the behaviors of B2 and B4, the total resistance of B5 cell only increases slightly from 30 to 180 service cycles (B5 to B5' in Table IV). An examination of the charge transfer resistance

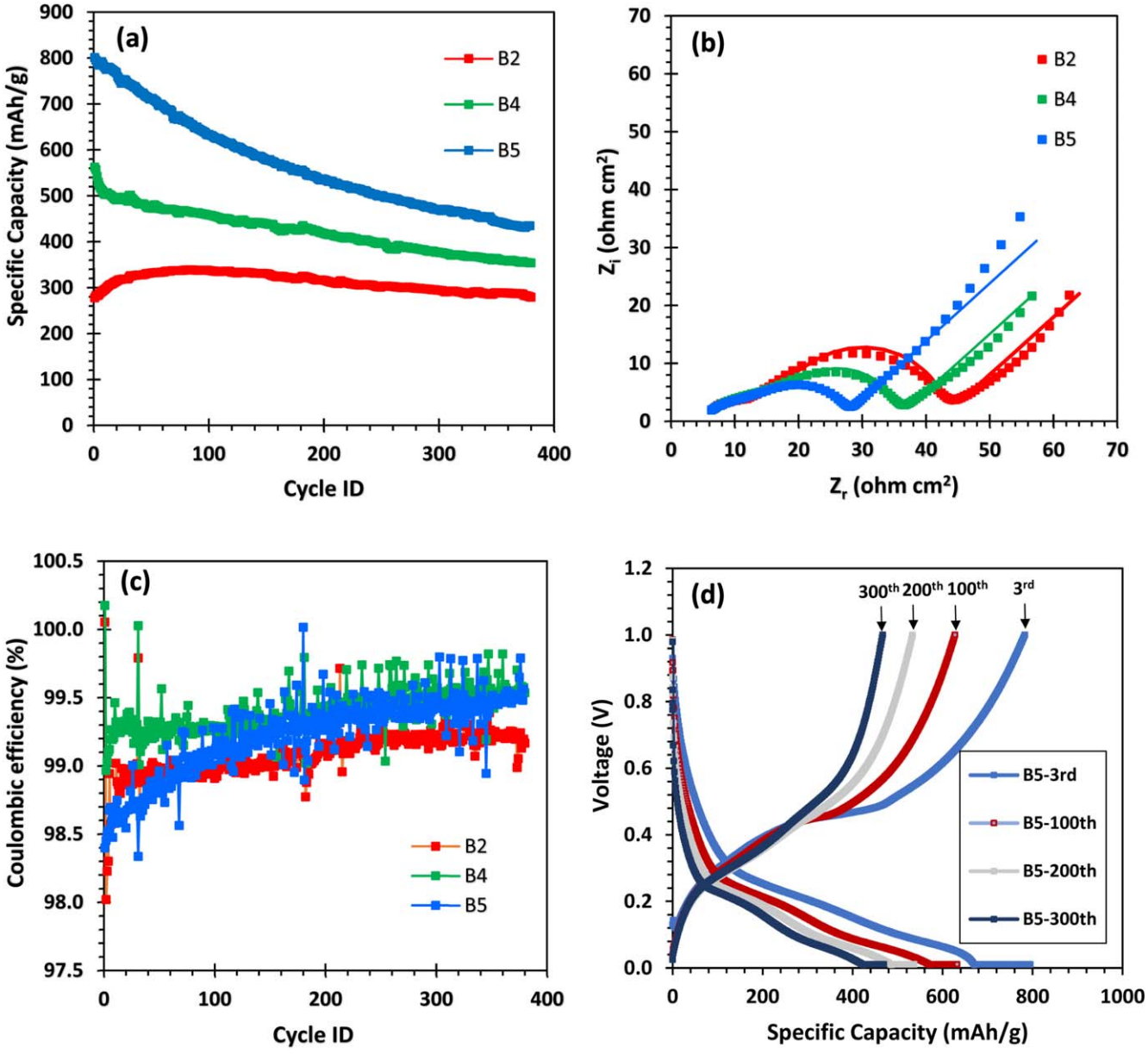


**Figure 9.** (a) Cycle stability comparison among B2, B4 and B5 cells (8:1:1 electrodes) with E5 electrolyte and P4, P5 and P6 charge/discharge protocols, respectively; (b) their electrochemical impedance spectra after 180 service cycles where dots are measured data and lines are fitted data using the equivalent circuit of R(CR)(CR)(C(RW)); (c) their coulombic efficiency as a function of cycle numbers; and (d) charge/discharge curves of selected cycles for B5 cells with E5 electrolyte and P6 protocol.

reveals that it also increases for B5 cell as the cycle number increases from 30 to 180, but the increase is smaller than B2 and B4 cells, suggesting that repeated fracture and formation of the SEI layer in B5 cell is not as frequent as in B2 and B4 cells. This trend is in good accordance with the fact that B5 cell has a lower cutoff voltage (0.01 V vs Li/$Li^+$) than B2 and B4 cells (0.1 V vs Li/$Li^+$) in the service cycles and thus has a more durable SEI layer and less frequent fracture and reformation of the SEI layer.

As discussed before, coulombic efficiency as a function of cycles can provide some insights towards the capacity decay processes. As shown in Fig. 9c, the average CE of B5 cell is low (< 99.0%) in the first 75 cycles after which its CE becomes higher than that of B2 cell. The average CE of B5 cell continuously increases as the cycle number increases beyond 75 cycles and at about 160 cycles becomes similar to that of B4 cell (∼99.3%). These trends can be explained as follows. The very low CE of B5 cell in the first 75 cycles indicate significant irreversible processes which are likely induced by two concurrent events, one being repeated fracture and formation of SEI layers and the other being fracture and thus loss of some Si@void@C particles in participation in redox reactions. Fracture and loss of some Si@void@C particles are more frequent when the lithiation cutoff voltage is at 0.01 V vs Li/$Li^+$ for B5 cell than at 0.1 V vs Li/$Li^+$ for B2 and B4 cells because the former has larger volume expansion than the latter.

Interestingly, the average CE of all cells improve as the cycle number increases. However, beyond 200 cycles the average CEs of all cells become stabilized with B2 having the lowest CE among three cells (Fig. 9c). These trends suggest that fracture and loss of the most favorable Si@void@C particles for redox reactions have reduced after 200 cycles beyond which the specific capacities of all cells are provided by the majority of Si@void@C particles that are still connected to the conductive carbon networks. Accompanied with the reductions in fracture and loss of Si@void@C particles, the specific capacity decay rate of B5 cell become similar to that of B4 cell beyond 200 cycles (Fig. 9a). The reason for B2 cell to have the lowest CE among three cells beyond 200 cycles is likely related to its least durable SEI layer among the three cells because B2 cell has a higher lithiation cutoff voltage than B4 cell in the formation cycles and B5 cell in all cycles.

Examination of charge/discharge curves of B5 cells (Fig. 9d) reveals that they are similar to those of B4 cells (Fig. 8d, i.e., the specific capacity from the CC segment is always larger than that from the CV segment and the capacities from both the CC and CV segments decrease as cycle number increases (Figs. S4 and S5). However, the specific capacity from the CC segment of B5 cells accounts for about 90% of the total capacity, whereas the CC segment of B4 cells only contributes about 74% of the total capacity. The difference is clearly due to different charge/discharge protocols because both cells have the same electrolyte (E5). The cutoff voltage of B5 cells in lithiation is 0.01 V vs Li/$Li^+$ (P6 in Table IV), whereas the corresponding value for B4 cells is 0.1 V vs Li/$Li^+$ (P5 in Table IV). The lower cutoff voltage of B5 cells in the CC segment results in much higher specific capacities from the CC segment and thus lower specific capacities from the CV segment. In addition, it is interesting to note that the percentage of the CC segment contribution to the specific capacity remains almost constant for both cells (such as 90.5% and 90.6% for B5 cells at the 100th and 300th cycles, and 73.8% and 73.5% for B4 cells at the 100th and 300th cycles, respectively). This trend indicates that the rate-sensitive capacity from the CC segment and the rate-non-sensitive capacity from the CV segment decrease in the same rate for Si@void@C with E5 electrolyte and P5 and P6 protocol. However, this is not the case for B2 cells with E5 electrolyte but P4 protocol, indicating a strong dependance of the capacity decay of Si@void@C with E5 on charge/discharge protocol.

Before closing, it is worth pointing out that in spite of capacity decay of B5 cell over 380 cycles, its specific capacity at the electrode level (including the consideration of CB and PAA weights) is still superior to that of graphite electrode at the 380th cycle. Specifically, the specific capacity of Si@void@C anodes at the electrode level is 348 mAh $g^{-1}$-Si@void@C+CB+PAA at the 380th cycle, which is higher than the typical specific capacity of graphite anodes (327 mAh $g^{-1}$-graphite+CB+PVDF) at the electrode level (assuming the specific capacity of graphite as 355 mAh $g^{-1}$-graphite and the electrode composition composed of 92 wt% graphite, 2 wt% CB and 6 wt% PVDF). As such, there are advantages in using Si@void@C anodes over graphite anodes if applications require only 380 cycles. It can be expected that future improvement in controlling the volume of engineered voids and thus minimizing the volume expansion of Si@void@C particles during lithiation can extend such an advantage of Si@void@C anodes to life beyond 380 cycles.

## Concluding Remarks

The impacts of five different electrolytes on the specific capacity and cycle stability of Si@void@C anodes have been investigated in this study. Two electrode compositions, i.e., 6:2:2 and 8:1:1 electrodes, have been evaluated as well. This study confirms that Gen2 electrolyte does offer higher specific capacities (∼40 mAh $g^{-1}$ higher) than Gen1 electrolyte in the first 200 cycles for Si@void@C electrodes. However, beyond 200 cycles the advantages of Gen2 electrolyte disappear. Moreover, beyond 300 cycles Gen1 electrolyte actually provides higher specific capacities (∼35 mAh $g^{-1}$ higher) than Gen2 electrolyte. These capacity trends coincide well with the different impedance changes over 400 cycles exhibited by the cells with Gen1 and Gen2 electrolytes, indicating that the SEI layers generated by Gen1 and Gen2 electrolytes have different impedances and cycle stabilities. This study also reveals that adding more FEC and VC additives to Gen2 electrolyte leads to higher cell impedance. In particular, the EC:DMC electrolyte with 10 vol% VC addition generates SEI layers with high impedances, but mechanically durable, thereby resulting in less fracture and loss of Si@void@C particles in electrochemical reactions and thus specific capacities as high as Gen2 electrolyte from 20 to 200 cycles. However, beyond 200 cycles the specific capacity of the cell with 10 vol% VC electrolyte suddenly decreases quickly, possibly due to sudden rupture of the durable SEI layers after enduring 200 charge/discharge and volume expansion/shrinkage cycles.

Electrolytes with a very high FEC concentration (FEC:DMC in 1:4 w/w) manifest strong dependance on the lithiation cutoff voltage. With the lower cutoff voltage at 0.01 V vs Li/$Li^+$ the cell impedance increases little from 30 to 180 service cycles (∼10% increase). In contrast, the cell impedance increases by ∼92% from 30 to 180 cycles when the lower cutoff voltage is at 0.1 V vs Li/$Li^+$. Interestingly, if the cutoff voltage is at 0.01 V vs Li/$Li^+$ in the formation cycles followed by the cutoff voltage at 0.1 V vs Li/$Li^+$ in the service cycles (P5 protocol), the cell impedance increase becomes smaller (only ∼41% increase) from 30 to 180 service cycles. All of these reveal that the SEI layers generated by the very high FEC electrolyte with the lower cutoff voltage at 0.01 V vs Li/$Li^+$ are very durable, thereby minimizing repeated fracture and reformation of SEI layers during cycles and thus little increase in the cell impedance as the cycle number increases. The understandings developed in this study offer critical guidelines for selection of electrolytes in conjunction with appropriate charge/discharge protocols and rational design of Si anodes to further improve the capacity and cycle stability of Si-based cells in the future.

## Acknowledgments

This work was supported by the U.S. National Science Foundation (NSF) with the award numbers CMMI-1660572 and IIP-1918991. LS is also grateful to the Rowe Family Endowment Fund.

## ORCID

Leon L. Shaw https://orcid.org/0000-0002-2170-1573

## References


1. H. Wu et al., "Stable cycling of double-walled silicon nanotube battery anodes through solid-electrolyte interphase control." *Nat. Nanotechnol.*, **7**, 310 (2012).
2. M. Ashuri, Q. He, and L. Shaw, "Silicon as a potential anode material for Li-ion batteries: where size, geometry and structure matter." *Nanoscale*, **8**, 74 (2016).
3. J. M. Martinez De La Hoz, F. A. Soto, and P. B. Balbuena, "Effect of the electrolyte composition on SEI reactions at Si anodes of Li ion batteries." *J. Phys. Chem. C*, **119**, 7060 (2015).
4. M. Nie et al., "Silicon solid electrolyte interphase (SEI) of lithium ion battery characterized by microscopy and spectroscopy." *J. Phys. Chem. C*, **117**, 13403 (2013).
5. Y. Jin, N.-J. H. Kneusels, L. E. Marbella, E. Castillo-Martínez, P. C.-M. M. Magusin, R. S. Weatherup, E. Jónsson, T. Liu, S. Paul, and C. P. Grey, "Understanding fluoroethylene carbonate and vinylene carbonate based electrolytes for Si anodes in lithium ion batteries with NMR spectroscopy." *J. Am. Chem. Soc.*, **140**, 9854 (2018).
6. Q. Li, X. Liu, X. Han, Y. Xiang, G. Zhong, J. Wang, B. Zheng, J. Zhou, and Y. Yang, "Identification of the solid electrolyte interface on the Si/C composite anode with FEC as the additive." *ACS Appl. Mater. Interfaces*, **11**, 14066 (2019).
7. M. Klett, J. A. Gilbert, K. Z. Pupek, S. E. Trask, and D. P. Abraham, "Layered oxide, graphite and silicon-graphite electrodes for lithium-ion cells: effect of electrolyte composition and cycling windows." *J. Electrochem. Soc.*, **164**, A6095 (2017).
8. H. Jia et al., "High-performance silicon anodes enabled by nonflammable localized high-concentration electrolytes." *Adv. Energy Mater.*, **9**, 1900784 (2019).
9. S. Yang et al., "Rational electrolyte eesign to form inorganic–polymeric interphase on silicon-based anodes." *ACS Energy Lett.*, **6**, 1811 (2021).
10. J. Chen et al., "Electrolyte design for LiF-rich solid-electrolyte interfaces to enable high-performance microsized alloy anodes for batteries." *Nat. Energy*, **5**, 386 (2020).
11. I. Yoon, S. Jurng, D. P. Abraham, B. L. Lucht, and P. R. Guduru, "Measurement of mechanical and fracture properties of solid electrolyte interphase on lithium metal anodes in lithium ion batteries." *Energy Storage Mater.*, **25**, 296 (2020).
12. J. Bareño, I. A. Shkrob, J. A. Gilbert, M. Klett, and D. P. Abraham, "Capacity fade and its mitigation in Li-ion cells with silicon-graphite electrodes." *J. Phys. Chem. C*, **121**, 20640 (2017).
13. T. Jaumann et al., "Lifetime vs rate capability: understanding the role of FEC and VC in high-energy Li-ion batteries with nano-silicon anodes." *Energy Storage Mater.*, **6**, 26 (2017).
14. V. Etacheri, O. Haik, Y. Goffer, G. A. Roberts, I. C. Stefan, R. Fasching, and D. Aurbach, "Effect of fluoroethylene carbonate (FEC) on the performance and surface chemistry of Si-nanowire Li-ion battery anodes." *Langmuir*, **28**, 965 (2011).
15. D. Pritzl, S. Solchenbach, M. Wetjen, and H. A. Gasteiger, "Analysis of vinylene carbonate (VC) as additive in graphite/$LiNi_{0.5}Mn_{1.5}O_4$ cells." *J. Electrochem. Soc.*, **164**, A2625 (2017).
16. G. M. Veith, M. Doucet, R. L. Sacci, B. Vacaliuc, J. K. Baldwin, and J. F. Browning, "Determination of the solid electrolyte interphase structure grown on a silicon electrode using a fluoroethylene carbonate additive." *Sci. Reports*, **7**, 6326 (2017).
17. W. Huang, J. Wang, M. R. Braun, Z. Zhang, Y. Li, D. T. Boyle, P. C. Mclntyre, and Y. Cui, "Dynamic structure and chemistry of the silicon solid-electrolyte interphase visulized by cryogenic electron microscopy." *Matter*, **1**, 1232 (2019).
18. M. Haruta, T. Okubo, Y. Masuo, S. Yoshida, A. Tomita, T. Takenaka, T. Doi, and M. Inaba, "Temperature effects on SEI formation and cyclability of Si nanoflake powder anode in the presence of SEI-forming additives." *Electrochim. Acta*, **224**, 186 (2017).
19. Y. Ha, C. Stetson, S. P. Harvey, G. Teeter, B. J. Tremolet de Villers, C.-S. Jiang, M. Schnabel, P. Stradins, A. Burrell, and S.-D. Han, "Effect of water concentration in $LiPF_6$-based electrolytes on the formation, evolution, and properties of the solid electrolyte interphase on Si anodes." *ACS Appl. Mater. Interfaces*, **12**, 49563 (2020).
20. E. Markevich et al., "Amorphous columnar silicon anodes for advanced high voltage lithium ion full cells: dominant factors governing cycling performance." *J. Electrochem. Soc.*, **160**, A1824 (2013).
21. Q. He, M. Ashuri, Y. Liu, B. Liu, and L. Shaw, "Silicon micro-reactor as a fast charge, long cycle life anode with high initial coulombic efficiency for Li-ion batteries." *ACS Appl. Energy Mater.*, **4**, 4744 (2021).
22. B. Liu, M. Luo, Z. Wang, C. Passolano, and L. Shaw, "On the specific capacity and cycle stability of Si@void@C anodes: effects of particle size and charge/discharge protocol." *Batteries*, **8**, 154 (2022).
23. L. Chen, H. Wu, X. Ai, Y. Cao, Z. Chen, and Z. Chen, "Toward wide-temperature electrolyte for lithium–ion batteries." *Battery Energy*, **1**, 20210006 (2022).
24. C. R. Yang, Y. Y. Wang, and C. C. Wan, "Composition analysis of the passive film on the carbon electrode of a lithium-ion battery with an EC-based electrolyte." *J. Power Sources*, **72**, 66 (1998).
25. M. Luo, M. T.-F. Rodrigues, L. Shaw, and D. P. Abraham, "Examining effects of negative to positive capacity ratio in three-electrode lithium-ion cells with layered oxide cathode and Si anode." *ACS Appl. Energy Mater.*, **5**, 5513 (2022).
26. S. Pidaparthy, M. Luo, M. T.-F. Rodrigues, J. M. Zuo, and D. P. Abraham, "Physicochemical heterogeneity in silicon anodes from cycled lithium-ion cells." *ACS Appl. Mater. Interfaces*, **14**, 38660 (2022).